International Immunopharmacology 72 (2019) 385–394

Contents lists available at ScienceDirect

International Immunopharmacology

journal homepage: www.elsevier.com/locate/intimp

Stemona alkaloids suppress the positive feedback loop between M2 polarization and fibroblast differentiation by inhibiting JAK2/STAT3 pathway in fibroblasts and CXCR4/PI_3K/AKT1 pathway in macrophages

Qi Ding, Jing Sun, Weina Xie, Mian Zhang*, Chaofeng Zhang, Xianghong Xu*

School of Traditional Chinese Pharmacy, China Pharmaceutical University, Nanjing 211198, Jiangsu, China

ARTICLE INFO

Keywords:
Pulmonary fibrosis
Stemona tuberosa
Macrophage
TGF-β1
Fibroblast
SDF-1

ABSTRACT

This study aimed to investigate the interaction between macrophages and fibroblasts in pulmonary fibrosis and the effects of total alkaloids of *Stemona tuberosa* (STA, 9 alkaloids with relative content of 91.2%) on them. The culture medium of LPS- or IL-4-induced macrophages was used as conditioned medium (CM) to co-culture with fibroblasts to study the effect of macrophages on the differentiation of fibroblasts. Similarly , the CM of TGF-β1-induced fibroblasts was co-culture with macrophages to study the effect of fibroblasts on the polarization of macrophages. The results showed that the TGF-β1 level in IL-4-induced (M2) rather than LPS-induced (M1) macrophages was significantly high ($p < 0.001$), and the SDF-1 level in TGF-β1-induced fibroblasts (MF) was significantly high ($p < 0.001$). The expressions of α-SMA and Col-1 in M2-CM-induced fibroblasts and Arg-1 and CXCR4 in MF-CM-induced macrophages were significantly increased ($p < 0.01$). STA effectively decreased the expressions of α-SMA ($p < 0.05$, 0.01 at 10, 100 μg/mL), Col-1 ($p < 0.05$, 0.05, 0.01 at 1, 10, 100 μg/mL), Arg-1 ($p < 0.01$ at 1, 10, 100 μg/mL) and CXCR4 ($p < 0.01$, 0.001 at 10, 100 μg/mL), which were consistent with the experimental results *in vivo*. These results suggested that there was a positive feedback loop between M2 polarization and fibroblast differentiation in pulmonary fibrosis. Further studies showed that the transcription of *sdf-1* gene in MF was initiated by JAK2/STAT3 pathway and the M2 polarization was promoted by SDF-1/CXCR4/PI_3K/AKT1 pathway. STA blocked the feedback loop by suppressing JAK2/STAT3 pathway in fibroblasts and CXCR4-PI_3K/AKT1 pathway in macrophages.

1. Introduction

Pulmonary fibrosis is a chronic progressive lung disease characterized by excessive deposition of extracellular matrix in lung tissue, resulting in irreversible decline in gas exchange function until death [1]. Pulmonary fibrosis, especially idiopathic pulmonary fibrosis, has a high morbidity and mortality and the median survival time after diagnosis is only 2–4 years [2]. Pulmonary fibrosis has no effective treatment drugs or therapies. Nintedanib and pirfenidone approved by the FDA in 2014 can alleviate symptoms and delay the process of pulmonary fibrosis, but cannot block the progression of pulmonary fibrosis [3]. In addition, most patients who take these two drugs for a long time have serious adverse reactions and obvious withdrawal symptoms [4].

It is generally believed that the persistent differentiation of fibroblasts (FB) into myofibroblasts (MF) triggered by abnormal repair of alveolar epithelial cells is the central node to pulmonary fibrosis [5]. TGF-β1 is one of the most powerful pro-fibrosis cytokines, which promotes FB proliferation, induces FB transformation and inhibits MF apoptosis through Smad pathway [6,7]. MF (*i.e.*, activated FB) are the direct executors of pulmonary fibrosis by secreting extracellular matrix (ECM) to induce collagen deposition in lung tissue. Besides, MF inhibit ECM degradation by high expression of tissue inhibitors of metalloproteinases (TIMPs) [8]. On the other hand, more and more studies have shown that macrophages are the main drives of tissue fibrosis [9,10]. Macrophages can be polarized into different phenotypes with different microenvironments, mainly including classically activated macrophages (M1) and alternatively activated macrophages (M2). M1, labeled by iNOS, can promote inflammation and antagonize fibrosis by secreting TNF-α, IL-1, IL-6, NO and MMPs. While M2, labeled by Arg-1, can resist inflammation and promote fibrosis by secreting TGF-β1, PDGF, MMP12 and TIMPs [11]. M2 can stimulate the differentiation of FB into MF by releasing TGF-β1 and promote the deposition of ECM. However, it is not clear whether fibroblast differentiation affects macrophage polarization.

* Corresponding authors at: School of Traditional Chinese Pharmacy, China Pharmaceutical University, #639 Longmian Road, Nanjing 211198, China.
E-mail addresses: herbs@cpu.edu.cn (M. Zhang), xuxh168@126.com (X. Xu).

https://doi.org/10.1016/j.intimp.2019.04.030
Received 5 March 2019; Received in revised form 8 April 2019; Accepted 14 April 2019
Available online 24 April 2019

The root of *Stemona tuberosa* Lour. (Stemonaceae) is one of the traditional Chinese medicines for treating lung diseases [12]. It is a commonly used drug in the prescription of Chinese medicines for the treatment of pulmonary fibrosis [13]. It is also the main drug (monarch drug) in Baibu Decoction, an antique compound prescription for the treatment of pulmonary fibrosis [14]. Our previous studies showed that alkaloids were the main active constituents contained in *S. tuberosa* [15]. In this paper, taking the total alkaloids of *S. tuberosa* (STA) as an example, the interaction between fibroblasts and macrophages was investigated, and the effects and mechanism of STA on BLM-induced pulmonary fibrosis was also studied.

2. Materials and methods

2.1. Reagents and antibodies

Bleomycin (BLM) was purchased from Zhejiang Hisun Pharmaceutical Co., Ltd. (Taizhou, China). Nintedanib (Nib, purity ≥99%) was obtained from Jinan Xuande Medical Technology Co., Ltd. (Jinan, China). MTT (3-(4,5-dimethylthiazol-2-yl)-2.5-diphenyltetrazolium bromide) was obtained from Biosharp, (Hefei, China). Primary rabbit antibodies against Col 1 (wl0088), α-SMA (wl02509), JAK2 (wl02188), Phospho-JAK2 (wl02997), STAT3 (wl01836), Phospho-STAT3 (wl03001), PI_3K p110 (wl03380), PI_3K p85 (wl02240), AKT1 (wl01652) and Phospho-AKT1 (wl03706) were purchased from Shenyang Wanleibio Co., Ltd. (Shenyang, China). Rabbit antibodies against GAPDH (AC002), iNOS (A0312), Arg-1 (A1847), CXCR4 (A12534), AKT2 (A0336) and Phospho-AKT2 (AP0305) were purchased from ABclonal Co., Inc. (Wuhan, China). The HRP-conjugated anti-rabbit IgG (H + L) (YFSA02) was purchased from Nanjing Yifeixue Biotechnology Co., Ltd. (Nanjing, China). Tyrphostin AG-490 (#14704) was purchased from Cell Signaling Technology, Inc. (Boston, USA). AMD3100 (ab120718) was purchased from Abcam (Cambridge, UK). All the other chemicals used in the experiments were commercial products of reagent grade.

2.2. Preparation and analysis of STA

2.2.1. Preparation of STA

The dried roots of *S. tuberosa* were purchased from Bozhou Medicinal Materials Market (Bozhou, China), and authenticated by one of authors, Prof. Mian Zhang. STA was prepared as described in our previous study [15]. Briefly, the roots were extracted in reflux 3 times with 95% ethanol for 1 h each time. The combined extract was concentrated in vacuum to no alcoholic taste, adjusted to pH 1–2 with 4% hydrochloric acid and centrifuged. The supernatant was adjusted to pH 9–10 with concentrated ammonia and extracted with chloroform. The chloroform extract was dried to obtain STA.

2.2.2. Chromatographic and mass spectrometric conditions

The chemical constituents of STA were analyzed on an Agilent series 1200 HPLC system equipped with a quaternary pump, a degasser, an autosampler and a column compartment (Palo Alto, CA, USA). The sample was separated on a C18 column (4.6 mm × 250 mm, 5 μm; YMC, Japan) eluted with a mixture of 0.1% formic acid (A) and acetonitrile (B) in the gradient as follows: 0–5 min, maintained at 10% B; 5–10 min, linearly increased to 20% B; 10–30 min, increased to 40% B; 30–35 min, maintained at 40% B; 35–40 min, increased to 60% B; 40–50 min, increased to 90% B and maintained at 90% B for 10 min. The flow rate was 1 mL/min and the column temperature was set at 30 °C.

The mass detection was performed on an Agilent 6520 Q-TOF mass spectrometer (Santa Clara, CA, USA) equipped with an electrospray ionization source in positive mode. Mass conditions were set as follows: nebulizer pressure, 35 psi; capillary voltage, 4000 V; fragmentor voltage, 100 V; drying gas (N2) flow, 8 L/min; drying gas temperature, 300 °C; collision energy, 40 V. The full-scan MS spectrum was recorded in *m/z* 100–1000 at a rate of 4 spectra/s, and the auto MS/MS spectra were recorded in m/z 50–1000 for 2 max precursors per cycle at a rate of 2 spectra/s. All data acquisition was controlled by Bruker Daltonics 4.1 software.

2.3. Animals

Adult male ICR mice (18–22 g, 6–8 weeks old) were purchased from Yangzhou University Comparative Medicine Center (Yangzhou, China). All mice were housed in a temperature- and humidity-controlled environment (25 °C, 60%) under a 12 h light/dark cycle and had free access to food and water. All the mice experiments were performed in accordance with the Guide for the Care and Use of Laboratory Animals and the related ethical regulations of China Pharmaceutical University, and the protocols was approved by the Institutional Ethical Committee of China Pharmaceutical University (SYXK (Su) 2013-0012, Nanjing, China). Mice were acclimatized for one week before experiments.

2.4. BLM-induced lung fibrosis and drug treatment

Weight-matched mice were randomly divided into five groups. After fasting for 12 h, mice were intratracheally administrated with BLM (3.5 U/kg in 0.9% NaCl) or 0.9% NaCl (sham) under anesthesia with 4% chloral hydrate (10 mL/kg) as described in the literature [16]. After 7 days of BLM treatment, STA (30 and 60 mg/kg) and Nib (30 mg/kg, positive drug) were administrated by gavage once a day for 14 days. Mice in sham and model group received an equivalent volume of 0.5% CMC-Na. On the 22nd day of BLM induction, mice were executed to collect serum and lungs. After weighing, a part of the lung tissue was fixed in 10% formalin over 24 h and embedded in paraffin for histological evaluation, and the rest was quickly frozen and stored at −80 °C.

2.5. Histopathological examination

Lung tissue sections (4–5 μm in thickness) were stained with hematoxylin and eosin (H&E) or Masson Trichrome. All sections were examined and assessed by professionals under light microscopy. Inflammation was scored from 0 (normal) to 5 (extremely severe damage) according to the degree of lung injury, including alveolar inflammation, congestion or bleeding of alveolar wall, proliferation of lymphocytes, emphysema, and degeneration or necrosis of bronchial epithelial cells. The collagen deposition in lung tissue was graded on a scale from 0 to 3 based on Masson Trichrome staining according to the degree of fibrous tissue proliferation.

2.6. Cell isolation and culture

Lung fibroblasts were isolated from BLM with/without STA-treated mice (for evaluating fibroblast differentiation) or untreated normal mice (for *in vitro* experiment, primary lung fibroblasts, PFB) by combining trypsin digestion and tissue adherent methods as described previously [17] and identified using vimentin immunohistochemical staining. Alveolar macrophages (for evaluating macrophage polarization) were isolated from BLM with/without STA-treated mice by bronchoalveolar lavage method. Briefly, the mouse trachea was lavaged several times with total 1 mL PBS (phosphate buffer solution) at room temperature. The lavage solution was centrifuged at 1500 rpm for 5 min, and the precipitation (alveolar cells) was washed twice with RPMI-1640 medium. Alveolar cells were seeded onto 6-well plates at about 1–5 × 10^5 cells/per well and incubated for 1–3 h, and then washed twice with PBS to removing dead cells. The mouse alveolar macrophage MH-S cell lines (for *in vitro* experiment) were purchased from Beijing Bnbio Research Institute (Beijing, China). PFB and MH-S cells were cultured in DMEM supplemented with 10% FBS and streptomycin

(100 mg/mL)/penicillin (100 U/mL) at 37 °C in a 5% CO_2 atmosphere.

2.7. MTT assay

Cells were seeded onto 96-well plates at about 1×10^5 cells/mL and incubated for 24 h (PFB) or 6 h (MH-S cells). After pretreatment with or without drugs for 48 h, 20 μL of MTT solution (5 mg/mL) were added into each well and the cells were incubated for 4 h. Formazan crystals were collected and dissolved with 150 μL of DMSO, and then measured at 490 nm with a microplate reader (Epoch, Bio-Tek, USA).

2.8. Fibroblast differentiation and macrophage polarization

PFB were seeded at about 5×10^5 cells/mL in 6-well plates. After 24 h of incubation, PFB were stimulated with 10 ng/mL of TGF-β1 (Peprotech, USA) and treated with drugs for 48 h. MH-S cells were seeded at about 5×10^5 cells/mL in 6-well plates. After 6 h of incubation, MH-S cells were stimulated with 0.5 μg/mL of LPS (Sigma-Aldrich, USA) or 10 ng/mL of IL-4 (Peprotech, USA) and treated with drugs for 48 h.

2.9. Preparation of conditioned medium

Conditioned medium (CM) were obtained from PFB induced with TGF-β1 and MH-S cells induced with LPS (M1) and IL-4 (M2). Cells were grown to subconfluence, then cultured in serum starvation for 48 h. Cell culture medium was collected and centrifuged, and the supernatant was used as CM (used freshly).

2.10. ELISA evaluation

The contents of TGF-β1 and SDF-1 in mouse serum and cell supernatants were determined by ELISA using commercial kits (Yifeixue Biotechnology, Nanjing, China) according to the manufacturer's protocols.

2.11. Western blot analysis

Immunoblot analysis of lung tissues or cells was performed on total lysates as described in literature [17] using primary antibodies mentioned in "*Reagents and antibodies*" and then incubated with corresponding secondary antibodies. The protein bands were detected by electrochemiluminescence (ECL) reagent (Tanon, Shanghai, China), and their intensity was quantitatively analyzed by using Image-Pro Plus software and presented as the ratio to GAPDH.

2.12. Quantitative real-time polymerase chain reaction (RT-PCR)

Total RNA of cells was extracted using TRIzol reagent (Yeasen, Shanghai, China) and reverse-transcribed to cDNA templates using an RT-MasterMix Kit (Vazyme, Nanjing, China). Quantitative RT-PCR was performed using SYBR Green Supermix (Bio-Rad, USA). Samples were measured in at least triplicate with a CFX96 real-time system (Bio-Rad, USA). The specific gene primers for *sdf-1*, *tgf-β1*, *arg-1*, *akt1* and *gapdh* were shown in Table 1. All the sample data were quantified using the comparative Ct method and presented as the mean ratio to *gapdh*.

2.13. Statistical analysis

All data were expressed as the mean ± SEM (standard error of mean) from at least three independent experiments. Statistical analysis of data was performed by one-way ANOVA followed by Student's two-tailed *t*-test by using GraphPad Prism 5 software. p values of < 0.05 were considered to be statistically significant.

3. Results

3.1. Effects of STA on BLM-induced pulmonary fibrosis in mice

The major constituents of STA were analyzed by HPLC-QTOF-MS method and their relative contents were evaluated based on the total ion current (TIC) chromatogram. As shown in Fig. 1A and S1 (in supplementary data), the 9 main peaks in TIC chromatogram were assigned as sessilifoline B (**1**, 8.5%), stemotinine (**2**, 4.7%), tuberostemonine J (**3**, 22.3%), croomine (**4**, 20.1%), isotuberostemonine (**5**, 4.9%), neotuberostemonine (**6**, 17.8%), tuberostemonine K (**7**, 1.7%), tuberospironine (**8**, 2.2%) and tuberostemonine (**9**, 9.0%). The total relative content of 9 alkaloids accounted for 91.2% of the total alkaloids.

The anti-pulmonary fibrosis effects of STA were evaluated in BLM-induced mice. Compared with the sham group, the mice in the model group showed significant decreases in survival rate (70%) (Fig. 1B) and body weight (Fig. 1C). However, STA treatment at doses of 30 and 60 mg/kg could increase the survival rate (75% and 87.5% for 30 and 60 mg/kg) and the weight of BLM-induced mice (Fig. 1B–C). The histopathological changes and the collagen deposition in lung tissues of mice were assessed by H&E staining and Masson's trichrome staining. Compared with the model group, STA treatment could decrease the infiltration of inflammatory cells, relieve the edema, thrombus and structure destruction (Fig. 1D) and also obviously decrease the collagen deposition (Fig. 1E). The inflammatory ($p < 0.05$ for both doses) and collagen ($p < 0.01$ for both doses) scores (Fig. 1F–G) evaluated by professionals were also significantly decrease after treatment with STA at 30 and 60 mg/kg. Moreover, the levels of TGF-β1 (a key pro-fibrotic cytokine) and SDF-1 (a chemokine which activates leukocytes) in mouse serum were analyzed by ELISA. As shown in Fig. 1H–I, the contents of TGF-β1 and SDF-1 in BLM-injured mice were obviously increased ($p < 0.001$), while STA treatment could significantly decrease the levels of TGF-β1 ($p < 0.05$ and 0.01 for 30 and 60 mg/kg) and SDF-1 ($p < 0.05$ and 0.01 for 30 and 60 mg/kg). In addition, the expression of CXCR4 protein, a specific receptor of SDF-1, was also determined by western blot. Compared with the sham group (Fig. 1J), the expression of CXCR4 in BLM-induced lung tissue was significantly increased ($p < 0.01$), however, STA treatment could obviously lower the elevated CXCR4 expression, especially at dose of 60 mg/kg ($p < 0.01$). These results were consistent with the previous experiments [15,16] and confirmed that STA could effectively inhibit BLM-induced pulmonary fibrosis.

3.2. Effects of STA on fibroblast differentiation and macrophage polarization in BLM-induced mice

The transformation of FB to MF is one of the key steps of pulmonary fibrosis. MF labeled with α-SMA [18] are the executors of pulmonary

Table 1
Sequences of real-time PCR primers.

Gene	Forward primer	Reverse primer
sdf-1	5′-TGCATCAGTGACGGTAAACCA-3′	5′-TTCTTCAGCCGTGCAACAATC-3′
tgf-β1	5′-CTCCCGTGGCTTCTAGTGC-3′	5′-GCCTTAGTTTGGACAGGATCTG-3′
arg-1	5′-CTCCAAGCCAAAGTCCTTAGAG-3′	5′-AGGAGCTGTCATTAGGGACATC-3′
akt1	5′-ATGAACGACGTAGCCATTGTG-3′	5′-TTGTAGCCAATAAAGGTGCCAT-3′
gapdh	5′-AGGTCGGTGTGAACGGATTTG-3′	5′-TGTAGACCATGTAGTTGAGGTCA-3′

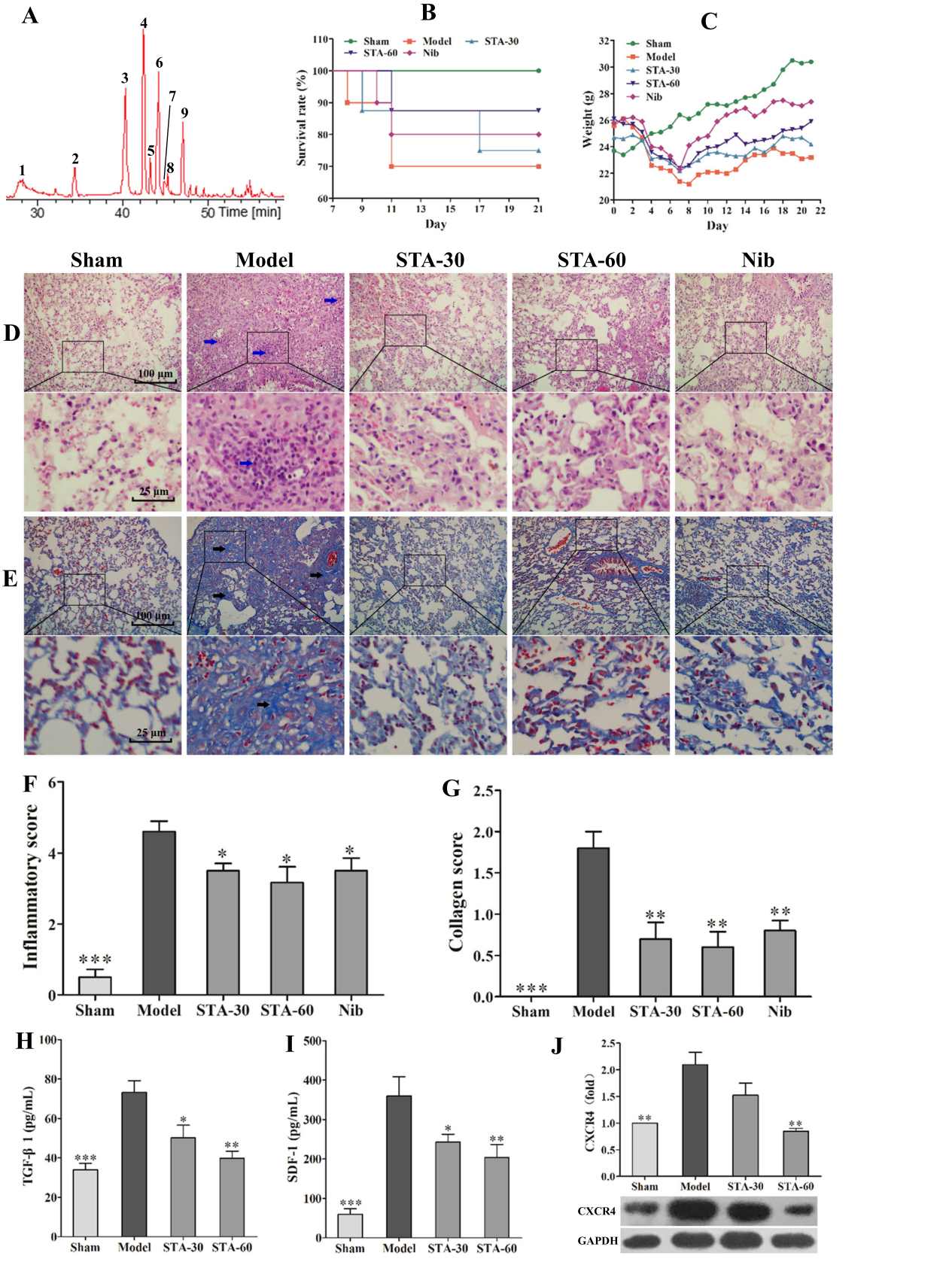

(caption on next page)

Fig. 1. Effects of STA on BLM-induced pulmonary fibrosis in mice. (A) Total ion current chromatogram (positive mode) of STA: sessilifoline B (**1**), stemotinine (**2**), tuberostemonine J (**3**), croomine (**4**), isotuberostemonine (**5**), neotuberostemonine (**6**), tuberostemonine K (**7**), tuberospironine (**8**), tuberostemonine (**9**). After 7 days of BLM (3.5 U/kg) treatment, mice were orally administrated with STA (30 and 60 mg/kg) and Nib (nintedanib, 30 mg/kg, positive drug) once a day for 14 days. (B) Cumulative survival rate of mice (n = 8–10); (C) changes of body weight of mice (n = 6–10); (D–G) H&E (blue arrow shows inflammatory infiltration) and Masson's trichrome (collagen deposition colored in blue and indicated by black arrow) staining section of lung tissue, and the inflammatory and collagen scores were assessed by professionals (n = 5); the levels of (H) TGF-β1 and (I) SDF-1 in serum were detected by ELISA (n = 3); (J) the expression of CXCR4 in lung tissue were detected by western blot (n = 3). Data were expressed as mean ± SEM, $*p < 0.05$, $**p < 0.01$, $***p < 0.001$, *versus* the model group. (For interpretation of the references to color in this figure legend, the reader is referred to the web version of this article.)

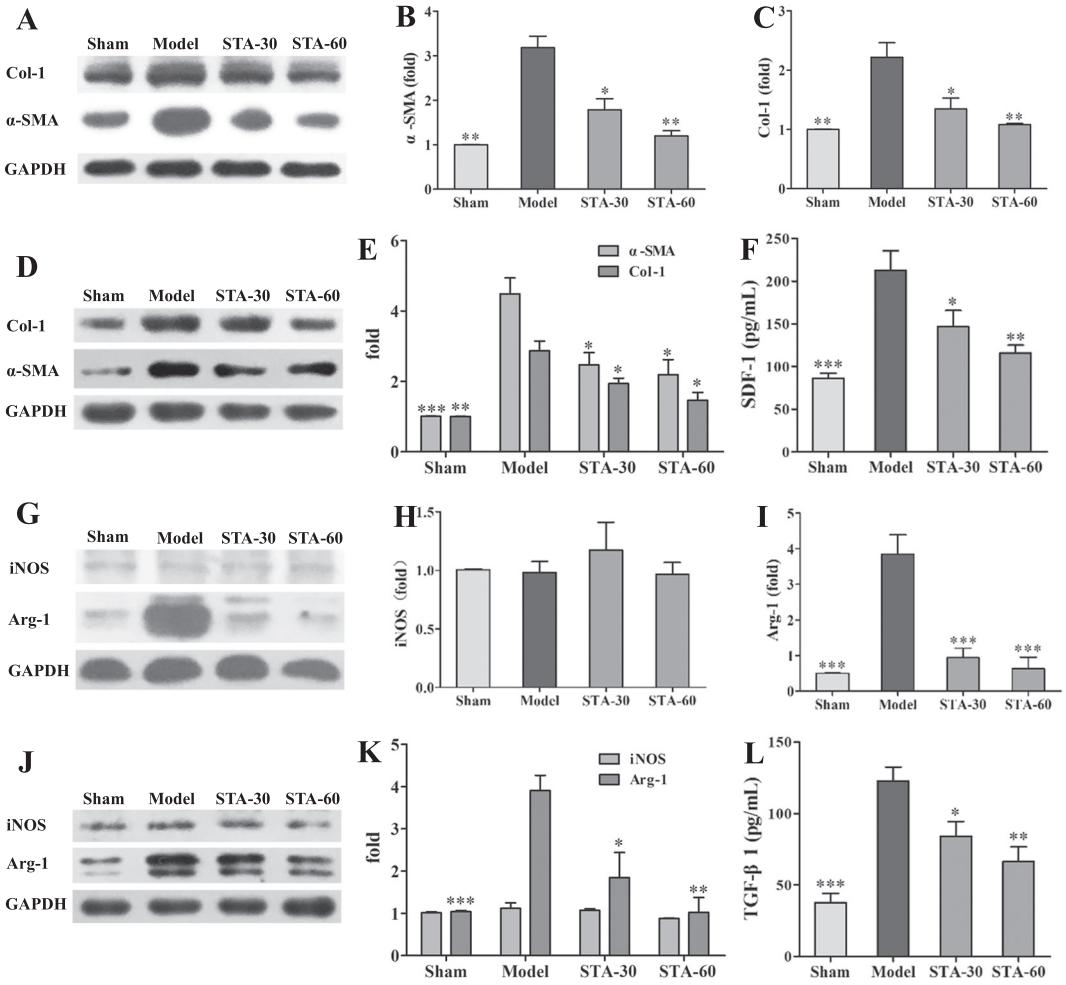

Fig. 2. Effects of STA on fibroblast differentiation and macrophage polarization in lung of BLM-induced mice. Mice were treated as described in Fig. 1. The expressions of α-SMA and Col-1 (A–C) in lung tissue and (D–E) in isolated fibroblasts were detected by western blot (n = 3), (F) the SDF-1 level in the culture medium of isolated fibroblasts was measured by ELISA (n = 3). The expressions of iNOS and Arg-1 (G–I) in lung tissue and (J–K) in isolated macrophages were detected by western blot (n = 3), (L) the TGF-β1 level in the culture medium of isolated macrophages was measured by ELISA (n = 3). Data were expressed as mean ± SEM, $*p < 0.05$, $**p < 0.01$, $***p < 0.001$, *versus* the model group.

fibrosis with the function of collagen secretion [19]. Therefore, the expressions of α-SMA and Col-1 in BLM-induced lung tissue and isolated lung FB of BLM-induced mice were evaluated by western blot. As shown in Fig. 2A–E, the levels of α-SMA and Col-1 in lung tissue (Fig. 2A–C) and isolated lung FB (Fig. 2D–E) of BLM-injured mice were significantly higher than that in the sham group ($p < 0.01$). Compared with the model group, STA treatment could reduce the levels of α-SMA ($p < 0.05$ and 0.01 for 30 and 60 mg/kg) and Col-1 ($p < 0.05$ and 0.01 for 30 and 60 mg/kg) in lung tissue, also reduce the levels of α-SMA ($p < 0.05$ for 30 and 60 mg/kg) and Col-1 ($p < 0.05$ for 30 and 60 mg/kg) in isolated lung FB. The results indicated that STA can inhibit the differentiation of FB into MF. Moreover, a high level of SDF-1 ($p < 0.001$) were detected in the culture medium of lung FB isolated from BLM-induced mice, and it was significantly lowered in that isolated from STA-treatment mice ($p < 0.05$ and 0.01 for 30 and 60 mg/kg) (Fig. 2F).

On the other hand, macrophages, including M1 and M2, are the regulators of pulmonary fibrosis. M1 labeled with inducible nitric oxide synthase (iNOS) have anti-inflammatory effects, while M2 labeled with Arginase-1 (Arg-1) have pro-fibrotic effects [20]. As shown in Fig. 2G–K, the expression of iNOS in lung tissue (Fig. 2G–I) and isolated alveolar macrophages (Fig. 2J–K) of BLM-injured mice was almost the same as that in the sham group, while the expression of Arg-1 was increased remarkably ($p < 0.001$ for both lung tissue and isolated alveolar macrophages), indicating that M2 were the dominant macrophage phenotype in BLM-induced lung tissues of mice. STA treatment significantly reduced the expression of Arg-1 in lung tissue ($p < 0.001$ for both 30 and 60 mg/kg) and isolated alveolar macrophages ($p < 0.05$ and 0.01 for 30 and 60 mg/kg). These results suggested that STA could effectively inhibit M2 polarization. Moreover, a significant

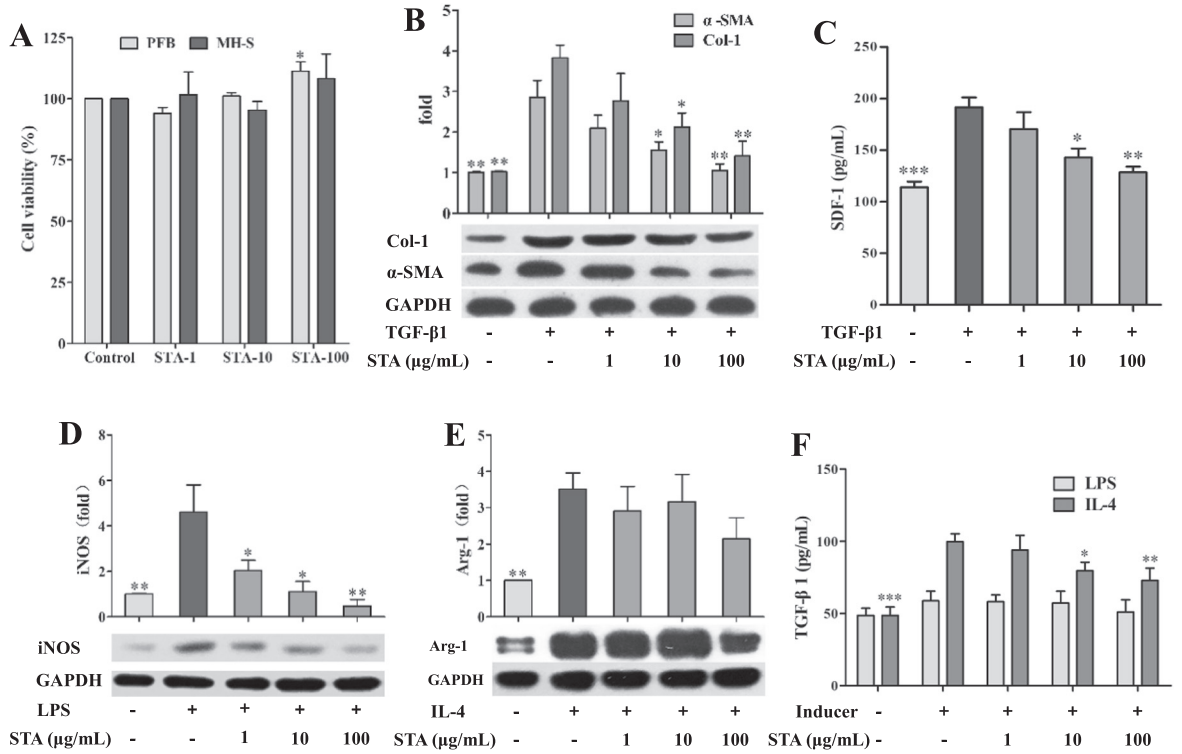

Fig. 3. Effects of STA on fibroblast differentiation and macrophage polarization *in vitro*. (A) PFB (mouse primary lung fibroblasts) and MH-S cells (mouse alveolar macrophages) were incubated with STA (1, 10, 100 μg/mL) for 48 h, cell viability was detected by MTT. (B-F) PFB cells were stimulated with TGF-β1 (10 ng/mL) and MH-S cells were stimulated with LPS (0.5 μg/mL) or IL-4 (10 ng/mL), and both PFB and MS-H cells were treated with STA (1, 10, 100 μg/mL) for 48 h. The expressions of (B) α-SMA, Col-1, (D-E) iNOS and Arg-1 were evaluated by western blot, (C) the SDF-1 level in the culture medium of PFB cells and (F) the TGF-β1 level in the culture medium of MH-S cells were measured by ELISA. Each experiment was repeated at least three times, and data were expressed as mean ± SEM, $^{*}p < 0.05$, $^{**}p < 0.01$, $^{***}p < 0.001$, *versus* the control (A) or the model (B–F) group.

high level of TGF-β1 ($p < 0.001$) were detected in the culture medium of alveolar macrophages isolated from BLM-induced mice, and it was significantly lowered in that isolated from STA-treatment mice ($p < 0.05$ and 0.01 for 30 and 60 mg/kg) (Fig. 2L).

3.3. Effects of STA on fibroblast differentiation and macrophage polarization in vitro

In vivo experiments showed that STA could improve BLM-induced pulmonary fibrosis in mice by inhibiting the FB differentiation and M2 polarization. However, it was not clear whether STA directly affected FB differentiation and M2 polarization. Therefore, primary lung FB (PFB) of mice and MH-S cells (a cell line of murine alveolar macrophages) were employed for the next experiments. The MTT assay showed that STA with concentration < 100 μg/mL had no cytotoxicity to PFB and MH-S cells (Fig. 3A).

The differentiation of FB into MF was induced by TGF-β1. As shown in Fig. 3B, the expressions of α-SMA and Col-1 in TGF-β1-induced PFB were increased significantly ($p < 0.01$ for both α-SMA and Col-1), while STA treatment at 1, 10 ($p < 0.05$) and 100 ($p < 0.01$) μg/mL reduced the levels of α-SMA and Col-1 in a concentration-dependent manner. This result was consistent with the *in vivo* experiment (Fig. 2D–E) and confirmed that STA could directly suppress TGF-β1-induced FB differentiation. Similarly (Fig. 2F), the SDF-1 level in the medium of TGF-β1-induced PFB was also significantly increased ($p < 0.001$) (Fig. 3C), suggesting that the activated FB (MF) are the main cells releasing SDF-1 to activate macrophages.

The M1 and M2 polarization were induced by LPS and IL-4, respectively. As shown in Fig. 3D and S2, the iNOS expression in LPS-stimulated MH-S cells were significantly increased ($p < 0.01$), but the expression of Arg-1 remained unchanged. The elevated expression could be significantly inhibited by STA treatment ($p < 0.05$, 0.05, 0.01 for 1, 10, 100 μg/mL) (Fig. 3D). This means that STA can directly block LPS-induced M1 polarization. Similarly, the Arg-1 expression in IL-4-induced MH-S cells was also significantly increased ($p < 0.01$), but the expression of iNOS remained unchanged (Fig. 3E and S2). Unlike the *in vivo* experiment (Fig. 2J–K), STA treatment could not reduce the Arg-1 level (Fig. 3E), suggesting that STA cannot inhibit IL-4-induced M2 polarization. The TGF-β1 levels in the medium of LPS- and IL-4-induced MH-S cells were determined by ELISA. As shown in Fig. 3F, the TGF-β1 level was increased significantly in MH-S cells induced by IL-4 ($p < 0.001$) rather than LPS. This was consistent with the *in vivo* experiment (Fig. 2L) and the report [21] that TGF-β1 is released by macrophages during M2 polarization.

3.4. Effects of STA on M2-macrophage induced fibroblast differentiation in vitro

It is known that TGF-β1 can directly induce the proliferation and differentiation of FB. However, macrophages, especially M2, are the main cells secreting TGF-β1 (Figs. 2L & 3F). Therefore, taking the supernatant of MH-S cells as conditioned medium (CM), the effects of M1 (LPS-induced) and M2 (IL-4-induced) on the differentiation of FB were studied. After treated with M1-CM or M2-CM for 48 h, the expression of α-SMA was only significantly increased in M2-CM-induced PFB ($p < 0.01$), and its intensity was similar to that induced by TGF-β1 (Fig. 4A). STA treatment (1, 10, 100 μg/mL) could remarkably decrease the expressions of α-SMA and Col-1 in M2-CM-induced PFB in a concentration-dependent manner (Fig. 4B). The results showed that M2 could directly promote the FB differentiation by secreting TGF-β1, and STA could significantly inhibit the FB differentiation.

As mentioned above, TGF-β1-induced fibroblasts (MF) may be the

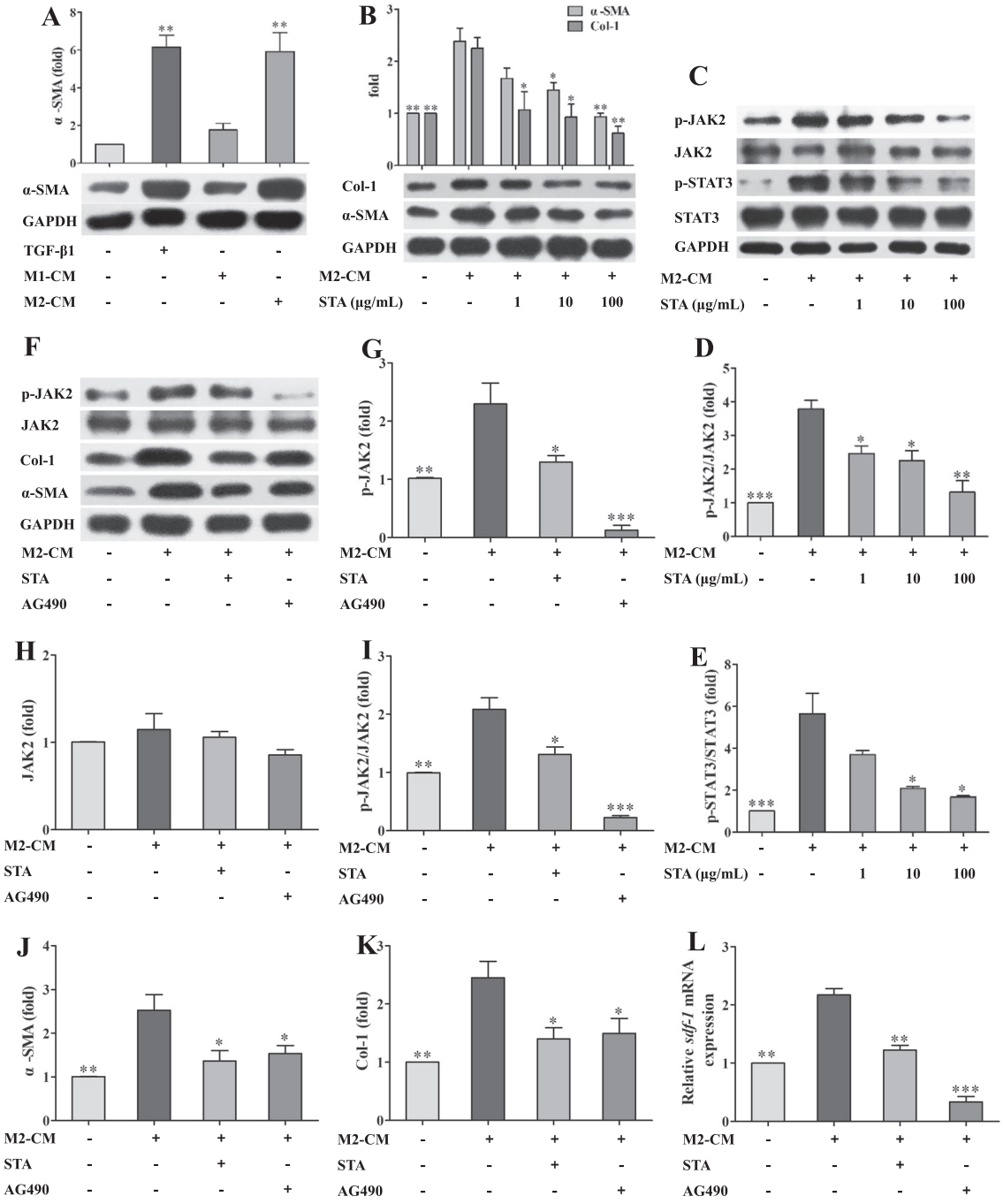

Fig. 4. Effects of STA on M2-macrophage induced fibroblast differentiation. (A) PFB were induced with the culture medium (as conditioned medium, CM) of MH-S cells stimulated by LPS (M1) or IL-4 (M2) for 48 h, taking TGF-β1 (10 ng/mL) as a positive control, the α-SMA level was detected by western blot. (B–E) PFB were stimulated with M2-CM and treated with STA (1, 10, 100 μg/mL) for 48 h, the expressions of α-SMA, Col-1, p-JAK2 and p-STAT3 were detected by western blot. (F–L) PFB were stimulated with M2-CM and treated with STA (10 μg/mL) or AG490 (10 μM) for 48 h, (F–K) the expressions of p-JAK2, JAK2, α-SMA and Col-1 was detected by western blot; (L) the mRNA expression of *sdf-1* was detected by RT-PCR. Each experiment was repeated at least three times, and data were expressed as mean ± SEM, *$p < 0.05$, **$p < 0.01$, ***$p < 0.001$, *versus* the control (A) or M2-CM (B–L) group.

main cells releasing SDF-1 (Figs. 2F & 3C). It is reported that p-STAT3 binds to the promoter of *sdf-1* gene and initiates transcription and translation [22]. Therefore, the role of JAK2/STAT3 pathway in M2-CM-induced FB was investigated. As shown in Fig. 4C–E, the expressions of p-JAK2 and p-STAT3 were significantly increased ($p < 0.001$ for the both) in M2-CM induced PFB, while the elevated expressions were suppressed by STA treatment (1, 10, 100 μg/mL) in a concentration-dependent manner. Tyrphostin AG-490 (AG490) is an inhibitor that inhibits the activation of STAT3 by selectively blocking JAK2 [23,24]. After co-culture with AG490, the expressions of p-JAK2 in M2-CM-induced PFB were decreased dramatically ($p < 0.05$) (Fig. 4F–I), and the expressions of α-SMA and Col-1 were also decreased ($p < 0.05$) (Fig. 4F, J & K). After co-culture with AG490, the mRNA expression of *sdf-1* (Fig. 4L) was significantly increased ($p < 0.01$) in M2-CM induced PFB, and AG490 or STA (10 μg/mL) treatment strongly or obviously decreased the *sdf-1* expression ($p < 0.001$, 0.01 for AG490, STA). It has been reported that there may be a "crosstalk" between TGF-β1 and JAK/STAT signaling pathways [25–27]. These results suggested that TGF-β1 could indirectly initiate the transcription of *sdf-1* gene in FB by activating JAK2/STAT3 signaling pathway through

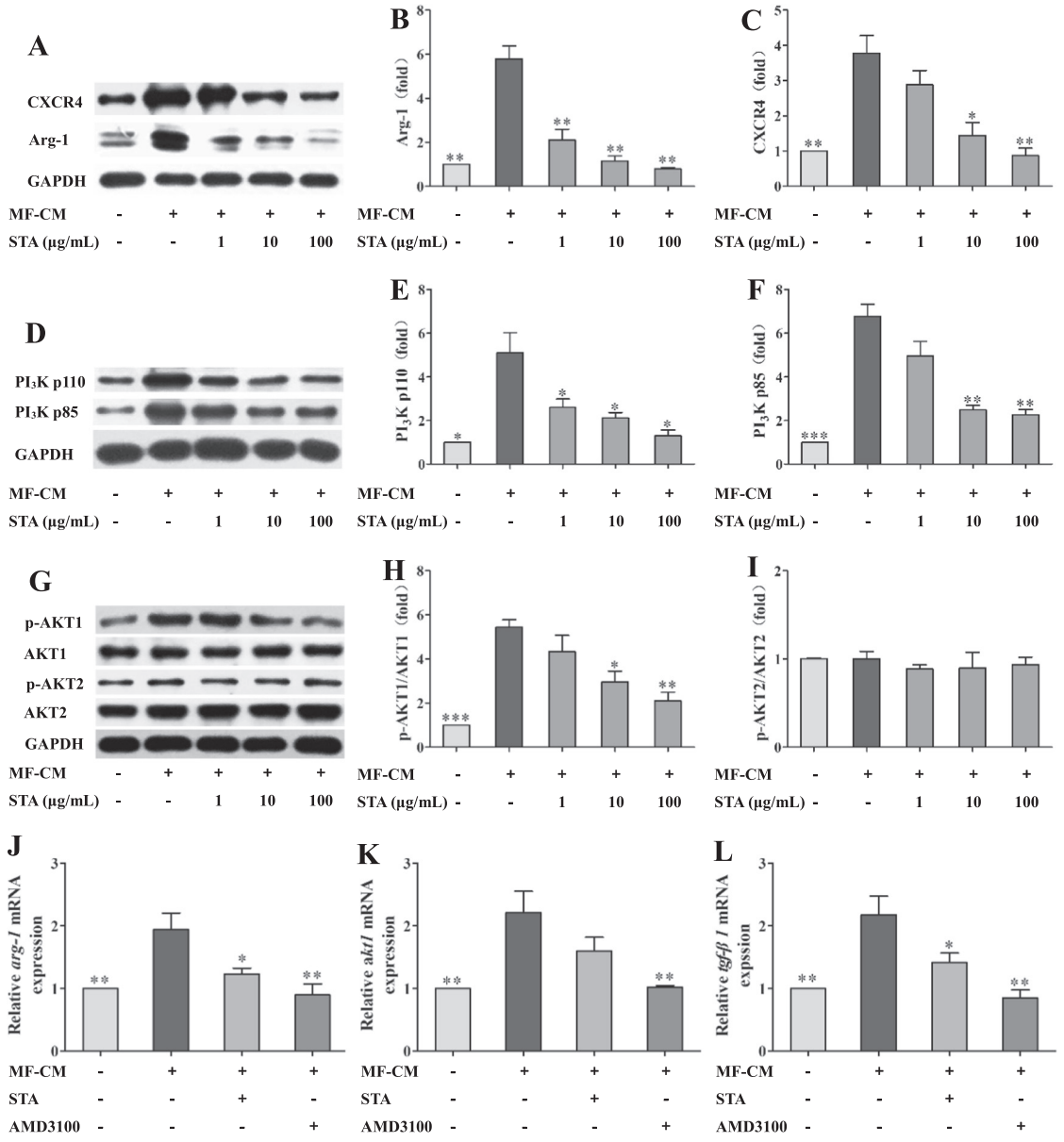

Fig. 5. Effects of STA on MF-induced M2 polarization of macrophages *in vitro*. (A–I) MH-S cells were induced with the culture medium of PFB stimulated by TGF-β1 (MF-CM) and treated with STA (1, 10, 100 μg/mL) for 48 h, the expressions of Arg-1, CXCR4, PI_3K p110, PI_3K p85, p-AKT1 and p-AKT2 were detected by western blot. (J–L) MH-S cells were induced with MF-CM and treated with STA (10 μg/mL) or AMD3100 (10 nM) for 48 h, the mRNA levels of *arg-1*, *akt1* and *tgf-β1* were detected by RT-PCR. Each experiment was repeated at least three times, and data were expressed as mean ± SEM, $*p < 0.05$, $**p < 0.01$, $***p < 0.001$, *versus* the MF-CM group.

a "crosstalk" mechanism. STA treatment could inhibit the *sdf-1* gene expression by blocking JAK2/STAT3 pathway and reduce the SDF-1 level in FB.

3.5. Effects of STA on myofibroblast-induced M2 polarization of macrophages in vitro

It was reported that SDF-1 has a strong chemotactic effect on macrophages and can induce their polarization [28]. The above experiments showed that pulmonary fibroblasts could secrete a large amount of SDF-1 during its differentiation (Fig. 3C). Therefore, the effects of MF (TGF-β1-induced fibroblasts) on the polarization of macrophages were studied using the supernatant of culture medium of MF as conditioned medium (MF-CM). After 48 h of MF-CM induction, the expressions of Arg-1 and CXCR4 in MH-S cells were significantly increased ($p < 0.01$ for both) (Fig. 5A–C), but the expression of iNOS remained unchanged (Fig. S2). Treatment with STA at 1, 10, 100 μg/mL dramatically decreased Arg-1 levels in MF-CM-induced MH-S cells ($p < 0.01$), and decreased CXCR4 levels in a concentration-dependent manner. The results suggested that MF could directly promote M2 polarization and STA inhibited M2 polarization by regulating SDF-1/CXCR4 axis.

The PI_3K/AKT pathway is one of the downstream pathways of CXCR4 and a key regulator of macrophage polarization. AKT1 and AKT2 play central but opposite roles in the control of macrophage phenotype [29,30]. Therefore, the main signals of PI_3K/AKT pathways in MF-CM-induced MH-S cells were evaluated by western blot. After 48 h of MF-CM induction, the expressions of PI_3K p110 and PI_3K p85 were significantly increased ($p < 0.05$) in MH-S cells, and these elevated expressions could be significantly reduced by treatment with STA at 1, 10, 100 μg/mL ($p < 0.05$) (Fig. 5D–F). For the AKT protein kinases, the level of p-AKT1 was significantly increased ($p < 0.001$) in

MF-CM-induced MH-S cells, while the level of p-AKT2 remained unchanged (Fig. 5G–I). STA treatment could decrease the level of p-AKT1 in a concentration-dependent manner (Fig. 5G & H). AMD3100 is an antagonist of CXCR4 [31]. After co-culture with AMD3100, the mRNA expressions of *arg-1*, *akt1* and *tgf-β1* in MF-CM-induced MH-S cells were significantly decreased ($p < 0.01$), and the effect of STA was similar to that AMD3100 (Fig. 5J–L). These results suggested that SDF-1/CXCR4 axis could promote M2 polarization by directly activating PI_3K/AKT1 pathway, thereby increasing the level of TGF-β1 in macrophages. STA could suppress M2 polarization by blocking PI_3K/AKT1 signaling pathway mediated by SDF-1/CXCR4 axis, thus reducing the release of TGF-β1 from macrophages.

4. Discussion

At present, it is generally believed that pulmonary fibrosis is the result of repeated abnormal repair of pulmonary epithelial tissue [32]. As regulators and executors of pulmonary fibrosis, macrophages and fibroblasts play extremely important roles in the occurrence and development of pulmonary fibrosis [8,10,33]. Although there are a lot of studies focusing on macrophages or fibroblasts, there are few studies on the interaction between macrophages and fibroblasts. In this paper, we confirmed that M2 could promote the transformation of FB into MF by secreting TGF-β1, while MF could induce M2 polarization by secreting SDF-1. Both of them formed a positive feedback loop, which may be one of the important reasons for the sustained development of pulmonary fibrosis. STA could alleviate BLM-induced pulmonary fibrosis by blocking the positive feedback loop between M2 and MF.

The positive regulation of M2 on FB differentiation is mainly achieved by secreting pro-fibrosis cytokines such as TGF-β1. TGF-β1 is recognized as the most important pro-fibrosis cytokine, which induces the transformation of FB into MF through the TGF-β1/Smad3 signaling pathway [34]. Consistently, the level of TGF-β1 in M2 macrophages was significantly higher than that in M1 or untreated (M0) macrophages (Figs. 2L & 3F). Accordingly, only M2-CM could stimulate the differentiation of FB into MF with the same intensity as TGF-β1 (Fig. 4A). These results indicated that M2 stimulated the transformation of FB to MF by secreting TGF-β1 and activating the TGF-β1/Smad3 signaling pathway. SDF-1 is mainly expressed in mesenchymal cells [35] and the level of SDF-1 was very high in TGF-β1-induced FB (*i.e.*, MF) (Figs. 2F & 3C), together with the high expressions of p-STAT3 and p-JAK2 (Fig. 4C–E). However, the high expressions of p-JAK2 protein and *sdf-1* mRNA in MF could be reversed by AG490, an inhibitor of JAK2 (Fig. 4G–I). Recent studies have shown that there is a “crosstalk” between TGF-β1/Smad and JAK2/STAT3 pathways in hepatic and pancreatic fibrosis [36,37]. These results showed that the transcription of *sdf-1* gene in MF is initiated by JAK2/STAT3 pathway, which may be activated by TGF-β1 through crosstalk mechanism. STA could suppress the transformation of FB into MF by inhibiting TGF-β1/Smad3 signaling pathway, and reduce the level of SDF-1 in MF by blocking JAK2/STAT3 signaling pathway.

It is not clear whether MF can regulate macrophage polarization in tissue fibrosis. It has been found that SDF-1 secreted by MF in prostate cancer can induce M2 polarization [28]. SDF-1 has a strong chemotaxis on lymphocytes [38]. High levels of Arg-1 and CXCR4 in MF-CM-induced MH-S cells (Fig. 5A–C) indicated that MF could induce M2 polarization and CXCR4 expression in macrophages. Activation of SDF-1/CXCR4 axis can activate downstream pathways such as PI_3K/AKT pathway. It was reported that the activation of AKT1 can promote M2 polarization, while the activation of AKT2 can promote M1 polarization [29,30]. In MF-CM-induced MH-S cells, the level of p-AKT1 rather than p-AKT2 was significantly increased (Fig. 5G–I). Moreover, the high mRNA expressions of *arg-1*, *akt1* and *tgf-β1* in MF-CM-induced MH-S cells could be reversed by AMD3100, an inhibitor of CXCR4 (Fig. 5J–L). These results suggested that MF induced M2 polarization through SDF-1/CXCR4/PI_3K/AKT1 pathway, thus promoting the TGF-β1 level in macrophages. STA suppress M2 polarization and TGF-β1 synthesis by inhibiting SDF-1/CXCR4/PI_3K/AKT1 signaling pathway. Interestingly, STA cannot inhibit the M2 polarization induced by IL-4 (Fig. 3E). This result suggested that the signal pathway of IL-4-induced M2 polarization (mainly through JAK/STAT6 pathway) is different from that of MF-CM-induced M2 polarization (mainly through PI_3K/AKT1 pathway mediated by SDF-1), and further study is needed.

In conclusion, our study suggested that there was a positive feedback loop between M2 polarization and FB differentiation in pulmonary fibrosis through TGF-β1 secreted by M2 and SDF-1 secreted by MF. STA could inhibit the secretion of SDF-1 and TGF-β1 by blocking JAK2/STAT3 in fibroblasts and CXCR4-PI_3K/AKT1 pathway in macrophages.

Conflict of interest

The authors declare that there are no conflicts of interest.

Acknowledgements

This work was funded by the National Natural Science Foundation of China (No. 81873075).

Appendix A. Supplementary data

Supplementary data to this article can be found online at https://doi.org/10.1016/j.intimp.2019.04.030.

References

[1] L. Richeldi, H.R. Collard, M.G. Jones, Idiopathic pulmonary fibrosis, Lancet 389 (2017) 1941–1952, https://doi.org/10.1016/S0140-6736(17)30866-8.
[2] B. Ley, H.R. Collard, T.E. King Jr., Clinical course and prediction of survival in idiopathic pulmonary fibrosis, Am. J. Respir. Crit. Care Med. 183 (2011) 431–440, https://doi.org/10.1164/rccm.201006-0894CI.
[3] G. Raghu, M. Selman, Nintedanib and pirfenidone. New antifibrotic treatments indicated for idiopathic pulmonary fibrosis offer hopes and raises questions, Am. J. Respir. Crit. Care Med. 191 (2015) 252–254, https://doi.org/10.1164/rccm.201411-2044ED.
[4] J.A. Galli, A. Pandya, M. Vega-Olivo, C. Dass, H. Zhao, G.J. Criner, Pirfenidone and nintedanib for pulmonary fibrosis in clinical practice: tolerability and adverse drug reactions, Respirology 22 (2017) 1171–1178, https://doi.org/10.1111/resp.13024.
[5] J. Liang, Y. Zhang, T. Xie, N. Liu, H. Chen, Y. Geng, A. Kurkciyan, J.M. Mena, B.R. Stripp, D. Jiang, P.W. Noble, Hyaluronan and TLR4 promote surfactant-protein-C-positive alveolar progenitor cell renewal and prevent severe pulmonary fibrosis in mice, Nat. Med. 22 (16) 1285–1293. doi:https://doi.org/10.1038/nm.4192.
[6] A. Leask, D.J. Abraham, TGF-beta signaling and the fibrotic response, FASEB J. 18 (2004) 816–827, https://doi.org/10.1096/fj.03-1273rev.
[7] K.C. Flanders, Smad3 as a mediator of the fibrotic response, Int. J. Exp. Pathol. 85 (2004) 47–64, https://doi.org/10.1111/j.0959-9673.2004.00377.x.
[8] C. Ramos C, M. Montaño, J. García-Alvarez, V. Ruiz, B.D. Uhal, M. Selman, A. Pardo, Fibroblasts from idiopathic pulmonary fibrosis and normal lungs differ in growth rate, apoptosis, and tissue inhibitor of metalloproteinases expression, Am. J. Respir. Cell Mol. Bio. 24 (2001) 591–598, https://doi.org/10.1165/ajrcmb.24.5.4333.
[9] A.J. Byrne, S.A. Mathie, L.G. Gregory, C.M. Lloyd, Pulmonary macrophages: key players in the innate defence of the airways, Thorax 70 (2015) 1189–1196, https://doi.org/10.1136/thoraxjnl-2015-207020.
[10] T.A. Wynn, L. Barron, Macrophages: master regulators of inflammation and fibrosis, Semin. Liver Dis. 30 (2010) 245–257, https://doi.org/10.1055/s-0030-1255354.
[11] P.J. Murray, Macrophage polarization, Annu. Rev. Physiol. 79 (2017) 541–566, https://doi.org/10.1146/annurev-physiol-022516-034339.
[12] National Pharmacopoeia Committee, Pharmacopoeia of People's Republic of China, Part 1, Chemical Industry Press, Beijing, 2015, pp. 132–133.
[13] J.S. Li, General situation of idiopathic pulmonary fibrosis treated by Chinese medicine, Acta Chin. Med. 32 (2017) 929–931, https://doi.org/10.16368/j.issn.1674-8999.2017.06.242.
[14] W.N. Xie, Q. Ding, J. Sun, C.F. Zhang, M. Zhang, X.H. Xu, Protective effects of Baibu Tang on bleomycin-induced pulmonary fibrosis in mice, J. China Pharm. Univ. 49 (2018) 483–489, https://doi.org/10.11665/j.issn.1000-5048.20180415.
[15] J. Xiang, P. Yu, M.D. Li, C.F. Zhang, X.H. Xu, M. Zhang, Protective effects of stemona alkaloids on mice with bleomycin-induced pulmonary fibrosis, J. China Pharm. Univ. 48 (2017) 76–81, https://doi.org/10.11665/j.issn.1000-5048.20170112.
[16] J. Xiang, S. Cheng, T.L. Feng, Y. Wu, W.N. Xie, M. Zhang, X.H. Xu, C.F. Zhang, Neotuberostemonine attenuates bleomycin-induced pulmonary fibrosis by suppressing the recruitment and activation of macrophages, Int. Immunopharmacol. 36 (2016) 158–164, https://doi.org/10.1016/j.intimp.2016.04.016.

[17] X.M. Lv, M.D. Li, S. Cheng, B.L. Liu, K. Liu, C.F. Zhang, X.H. Xu, M. Zhang, Neotuberostemonine inhibits the differentiation of lung fibroblasts into myofibroblasts in mice by regulating HIF-1α signaling, Acta Pharmacol. Sin. 39 (2018) 1501–1512, https://doi.org/10.1038/aps.2017.202.
[18] A.F. Muro, F.A. Moretti, B.B. Moore, M. Yan, R.G. Atrasz, C.A. Wilke, K.R. Flaherty, F.J. Martinez, J.L. Tsui, D. Sheppard, F.E. Baralle, G.B. Toews, E.S. White, An essential role for fibronectin extra type III domain a in pulmonary fibrosis, Am. J. Respir. Crit. Care Med. 177 (2008) 638–645, https://doi.org/10.1164/rccm.200708-1291OC.
[19] B. Hinz, Myofibroblasts, Exp. Eye Res. 142 (2016) 56–70, https://doi.org/10.1016/j.exer.2015.07.009.
[20] A.J. Byrne, T.M. Maher, C.M. Lloyd, Pulmonary macrophages: a new therapeutic pathway in fibrosing lung disease, Trends Mol. Med. 22 (2016) 303–316, https://doi.org/10.1016/j.molmed.2016.02.004.
[21] J.L. Larson-Casey, J.S. Deshane, A.J. Ryan, V.J. Thannickal, A.B. Carter, Macrophage Akt1 kinase-mediated mitophagy modulates apoptosis resistance and pulmonary fibrosis, Immunity 44 (2016) 582–596, https://doi.org/10.1016/j.immuni.2016.01.001.
[22] Y.Y. Li, H. Li, Z.L. Liu, Q. Li, H.W. Qiu, L.J. Zeng, W. Yang, X.Z. Zhang, Z.Y. Li, Activation of STAT3-mediated CXCL12 up-regulation in the dorsal root ganglion contributes to oxaliplatin-induced chronic pain, Mol. Pain 13 (2017) 1–11, https://doi.org/10.1177/1744806917747425.
[23] V. Palagani, P. Bozko, M. El Khatib, H. Belahmer, N. Giese, B. Sipos, N.P. Malek, R.R. Plentz, Combined inhibition of Notch and JAK/STAT is superior to monotherapies and impairs pancreatic cancer progression, Carcinogenesis 35 (2014) 859–866, https://doi.org/10.1093/carcin/bgt394.
[24] J. Damm, L.M. Harden, R. Gerstberger, J. Rotha, C. Rummel, The putative JAK-STAT inhibitor AG490 exacerbates LPS-fever, reduces sickness behavior, and alters the expression of pro- and anti-inflammatory genes in the rat brain, Neuropharmacology 71 (2013) 98–111, https://doi.org/10.1016/j.neuropharm.2013.03.014.
[25] B. Wang, T. Liu, J.C. Wu, S.Z. Luo, R. Chen, L.G. Lu, M.Y. Xu, STAT3 aggravates TGF-β1-induced hepatic epithelial-to-mesenchymal transition and migration, Biomed. Pharmacother. 98 (2018) 214–221, https://doi.org/10.1016/j.biopha.2017.12.035.
[26] R.Y. Liu, Y. Zeng, Z. Lei, L. Wang, H. Yang, Z. Liu, J. Zhao, H.T. Zhang, JAK/STAT3 signaling is required for TGF-β-induced epithelial-mesenchymal transition in lung cancer cells, Int. J. Oncol. 44 (2014) 1643–1651, https://doi.org/10.3892/ijo.2014.2310.
[27] K.D. Ju, J.W. Lim, K.H. Kim, H. Kim, Potential role of NADPH oxidase-mediated activation of Jak2/Stat3 and mitogen-activated protein kinases and expression of TGF-β1 in the pathophysiology of acute pancreatitis, Inflamm. Res. 60 (2011) 791–800, https://doi.org/10.1007/s00011-011-0335-4.
[28] G. Comito, E. Giannoni, C.P. Segura, P. Barcellos-de-Souza, M.R. Raspollini, G. Baroni, M. Lanciotti, S. Serni, P. Chiarugi, Cancer-associated fibroblasts and M2-polarized macrophages synergize during prostate carcinoma progression, Oncogene 33 (2014) 2423–2431, https://doi.org/10.1038/onc.2013.191.
[29] E. Vergadi, E. Ieronymaki, K. Lyroni, K. Vaporidi, C. Tsatsanis, Akt signaling pathway in macrophage activation and M1/M2 polarization, J. Immunol. 198 (2017) 1006–1014, https://doi.org/10.4049/jimmunol.1601515.
[30] A. Arranz, C. Doxaki, E. Vergadi, Y. Martinez de la Torre, K. Vaporidi, E.D. Lagoudaki, E. Ieronymaki, A. Androulidaki, M. Venihaki, A.N. Margioris, E.N. Stathopoulos, P.N. Tsichlis, C. Tsatsanis, Akt1 and Akt2 protein kinases differentially contribute to macrophage polarization, Proc. Natl. Acad. Sci. U. S. A. 109 (2012) 9517–9522, https://doi.org/10.1073/pnas.1119038109.
[31] E. De Clercq, AMD3100/CXCR4 inhibitor, Front. Immunol. 6 (2015) 276, , https://doi.org/10.3389/fimmu.2015.00276.
[32] Z.W. Cao, R. Lis, M. Ginsberg, D. Chavez, K. Shido, S.Y. Rabbany, G.H. Fong, T.P. Sakmar, S. Rafii, B.S. Ding, Targeting of the pulmonary capillary vascular niche promotes lung alveolar repair and ameliorates fibrosis, Nat. Med. 22 (2016) 154–162, https://doi.org/10.1038/nm.4035.
[33] N. Xie, Z. Tan, S. Banerjee, H.C. Cui, J. Ge, R.M. Liu, K. Bernard, V.J. Thannickal, G. Liu, Glycolytic reprogramming in myofibroblast differentiation and lung fibrosis, Am. J. Respir. Crit. Care Med. 192 (2015) 1462–1474, https://doi.org/10.1164/rccm.201504-0780OC.
[34] S.Y. Wang, X.X. Zhao, S.X. Yang, B.P. Chen, J. Shi, Knockdown of NLRC5 inhibits renal fibroblast activation via modulating TGF-β1/Smad signaling pathway, Eur. J. Pharmacol. 829 (2018) 38–43, https://doi.org/10.1016/j.ejphar.2018.03.045.
[35] R. Horuk, Chemokines beyond inflammation, Nature 393 (1998) 524–525, https://doi.org/10.1038/31116.
[36] J.H. Yu, K.H. Kim, H. Kim, SOCS 3 and PPAR-gamma ligands inhibit the expression of IL-6 and TGF-beta1 by regulating JAK2/STAT3 signaling in pancreas, Int. J. Biochem. Cell Biol. 40 (2008) 677–688, https://doi.org/10.1016/j.biocel.2007.10.007.
[37] T. Yamamoto, T. Matsuda, A. Muraguchi, K. Miyazono, M. Kawabata, Cross-talk between IL-6 and TGF-beta signaling in hepatoma cells, FEBS Lett. 492 (2001) 247–253, https://doi.org/10.1016/S0014-5793(01)02258-X.
[38] N. Arimitsu, J. Shimizu, N. Fujiwara, K. Takai, E. Takada, T. Kono, Y. Ueda, T. Suzuki, N. Suzuki, Role of SDF1/CXCR4 interaction in experimental hemiplegic models with neural cell transplantation, Int. J. Mol. Sci. 13 (2012) 2636–2649, https://doi.org/10.3390/ijms13032636.